



OPEN Desert dust improves the photophysiology of heat-stressed corals beyond iron

Katherine Amorim¹✉, R. Grover¹, D. Omanović², L. Sauzéat^{3,4},
M. I. Marcus Do Noscimiento¹, Maoz Fine^{5,6} & Christine Ferrier-Pagès¹✉

Desert dust is an important source of essential metals for marine primary productivity, especially in oligotrophic systems surrounded by deserts, such as the Red Sea. However, there are very few studies on the effects of dust on reef-building corals and none on the response of corals to heat stress. We therefore supplied dust to two coral species (*Stylophora pistillata* and *Turbinaria reniformis*) kept under control conditions (26 °C) or heat stress (32 °C). Since dust releases large amounts of iron (Fe) in seawater, among other metals, the direct effect of different forms of Fe enrichment on coral photosynthesis was also tested. First, our results show that the desert dust altered the coral metallome by increasing the content of metals that are important for coral physiology (e.g. lithium (up to 5-fold), manganese (up to 4-fold in *S. pistillata*), iron (up to 3-fold in *S. pistillata*), magnesium (up to 1.3-fold), molybdenum (up to 1.5-fold in *S. pistillata*)). Overall, metal enrichment improved the photosynthetic performance of corals, especially under thermal stress (e.g. Pgross (up to 2-fold), Pnet (up to 10-fold), chlorophyll (up to 1.5-fold), symbionts (up to 1.6-fold)). However, Fe exposure (ferric chloride or ferric citrate) did not directly improve photosynthesis, suggesting that it is the combination of metals released by the dust, the so-called “metal cocktail effect”, that has a positive impact on coral photophysiology. Dust also led to a decrease in Ni uptake (up to 1.4-fold in the symbionts), likely related to the nitrogen metabolism. Finally, we found that the isotopic signature of metals such as iron, zinc and copper is a good indicator of heat stress and dust exposure in corals. In conclusion, desert dust can increase coral resistance to bleaching by supplying corals with essential metals.

Keywords Bleaching, Iron, Manganese, Stable isotopes, Copper, Zinc

Mutualistic symbioses are widespread in both terrestrial and aquatic environments, with interactions between partners forming larger functional units (referred to as holobionts). These synergistic relationships allow holobionts to thrive in unfavorable environments¹. For example, corals form complex symbioses with various microorganisms, that enable them to build huge reef structures in oligotrophic reef waters². This symbiosis is based on efficient nutrient recycling between the partners: Symbiodiniaceae dinoflagellates³ perform photosynthesis and transfer photosynthetic products to the coral hosts, while the dinoflagellates receive nutrients from the metabolic and catabolic waste of the coral host^{4–6}. The stability of the symbiosis is crucial for the health of corals and the associated coral reefs. However, natural and anthropogenic disturbances, such as global warming, can disrupt the symbiosis, and lead to coral bleaching and widespread mortality^{7,8}.

Like all living organisms, corals and their associated microorganisms require both macro- and microelements for growth, reproduction, and adaptive responses^{9,10}. The acquisition, distribution and overall requirements of corals for macronutrients such as carbon, nitrogen and phosphorus have been studied for several decades and are becoming better understood¹⁰. In contrast, the role of micronutrients, particularly metals, in coral health and productivity is less well understood. However, metals are cofactors of several enzymes involved in photosynthesis, respiration, macronutrient acquisition and oxidative stress metabolism⁹, and Symbiodiniaceae

¹Coral Ecophysiology team, Centre Scientifique de Monaco, Principality of Monaco, 8 Quai Antoine 1 er, Monaco 98000, Principality of Monaco. ²Center for Marine and Environmental Research, Ruđer Bošković Institute, Bijenička cesta 54, Zagreb 10000, Croatia. ³Université Clermont Auvergne, CNRS, IRD, OPGC, Laboratoire Magmas et Volcans, Clermont-Ferrand 63000, France. ⁴Université Clermont Auvergne, CNRS, INSERM, Institut Génétique, Reproduction et Développement, Clermont-Ferrand 63000, France. ⁵Department of Ecology, Evolution and Behavior, The Alexander Silberman Institute of Life Sciences, The Hebrew University of Jerusalem, Jerusalem, Israel. ⁶The Interuniversity Institute for Marine Sciences in Eilat, P.O.B. 469, Eilat 88103, Israel. ✉email: kathyamorimbio@gmail.com; ferrier@centrescientifique.mc

have higher metal requirements compared to other phytoplankton groups^{11,12}. Some studies have therefore emphasized the importance of these metals for the stability of the coral-dinoflagellate symbiosis, using the coral *Stylophora pistillata* as a model. Iron deficiency exacerbated the susceptibility of this coral to bleaching during heat stress¹³, while metal supplementation through zooplankton feeding increased its resistance to heat stress¹⁴. Calcification of *S. pistillata* was increased under manganese enrichment¹⁵, while symbiotic photosynthesis and chlorophyll content were enhanced by a mixture of metals leached from desert dust or volcanic ash^{16,17}.

Corals from the Red Sea are naturally exposed to large amounts of metals due to the high deposition of desert dust¹⁸, which is the most important aerosol source of aluminium (Al), titanium (Ti), iron (Fe), manganese (Mn) and secondarily copper (Cu) and zinc (Zn)¹⁹. Desert dust is therefore a natural and valuable example of a “metal cocktail” that can help us understand the response of corals to metal exposure. However, only one study¹⁶ has investigated the effects of desert dust on corals. Although it has shown increased photosynthetic rates in the species *S. pistillata* exposed to desert dust, many questions remain unanswered. For example, as different Symbiodiniaceae species have different metal requirements¹², the effect of dust exposure on coral physiology could be species-specific. It is also not yet known whether the metals supplied by dust reduce or increase coral bleaching under heat stress. While dust can release metals that are known to have a positive effect on primary productivity (i.e. Fe, Zn, Mn)^{13–17}, it can also release other, potentially more toxic metals (i.e. Cu, As, Ti)²⁰.

In this study, we investigated the effects of desert dust on the ecophysiology of two Red Sea coral species (*Stylophora pistillata* and *Turbinaria reniformis*) kept either under control conditions (26 °C) or under heat stress (32 °C), to assess if those effects are species specific and temperature dependent. We first hypothesized that each coral holobiont will respond differently to dust exposure depending on its physiological needs. We then hypothesized that dust could increase the coral resistance to heat stress under our experimental conditions, if important elements such as manganese and iron can support coral photosynthesis¹⁵. Since dust is a cocktail of different metals, we also conducted an additional experiment in which corals were exposed to ferric chloride and ferric citrate to test the direct effects of iron alone on their rates of photosynthesis. We hypothesized that iron, which is often a limiting nutrient for corals, will improve coral photosynthesis under iron enrichment. To answer these questions, we measured several indicators of coral photosynthetic performance, including gross and net photosynthesis, and electron transport rate. We also measured chlorophyll concentrations, symbiont density, oxidative stress markers (total antioxidant capacity, catalase and glutathione peroxidase activities), and the metal content in the host and symbiont tissues. We performed stable isotope analysis ($\delta^{66}\text{Zn}$, $\delta^{56}\text{Fe}$ and $\delta^{65}\text{Cu}$) given that metal isotope ratios have been proved to be a good proxy of physiological stress in corals¹⁴. Altogether, the results will help to understand how the resistance of corals to heatwaves can be improved by metal supplementation.

Materials and methods

Dust experiment

Dust experimental setting

The experiments were performed with nubbins of the scleractinian corals *Stylophora pistillata* and *Turbinaria reniformis* grown in indoor aquaria at the Centre Scientifique de Monaco. The coral colonies were maintained in open-flow seawater at 26 °C and 200 $\mu\text{moles photons m}^{-2} \text{ s}^{-1}$ (12:12 light: dark) without dust provision. After being prepared, nubbins were maintained for 3 weeks at the above control conditions for acclimatization and fed twice weekly with *Artemia salina* nauplii.

160 nubbins of *S. pistillata* from five different colonies and 96 nubbins of *T. reniformis* were evenly distributed among eight 12 L aquaria (20 nubbins *S. pistillata* + 12 *T. reniformis* per aquaria). The aquaria were divided into four sets of two aquaria for each experimental condition (26 °C + dust; 26 °C + \emptyset (no dust); 32 °C + dust; 32 °C + \emptyset) and kept under a photosynthetically active radiation (PAR) of $180 \pm 20 \mu\text{mol photons m}^{-2} \text{ s}^{-1}$ (12:12 h photoperiod). From the first day of the experiment, the temperature in the 32 °C condition (with or without dust provision) was increased relatively slowly (0.5 °C every two days) from 26 °C to 32 °C, a temperature slightly above the upper level of the summer temperature in the Gulf of Aqaba²¹. To maintain a stable temperature, each of the 12 L tanks was kept inside a 25 L tank equipped with a thermostat, a heater and continuous flow of seawater. The 12 L and the 25 L tanks had an open water system that circulated between the two tanks, and both had a water pump for an efficient water circulation. Every day, the water exchange between the two aquaria was closed for six hours during the day and the tanks under dust condition received 1.25 mg L⁻¹ of desert dust every morning. The procedure was repeated four times a week. The dust used is the same as in Blanckaert et al.¹⁶ and was collected as Kessler et al.²², directly at the Inter-University Institute (Eilat, Gulf of Aqaba, Red Sea) and a few meters from the reef and from the desert. It was not necessary to sieve the dust because particles were of microscopic size (powderlike), clearly smaller than 200 μm and devoid of any large particle (e.g. fibers). The daily concentration of dust provided was slightly higher in our study because we provided it only 4 times per week, but the weekly quantity is the same as Blanckaert et al.¹⁶. Ninety milligrams of dust were pre-dissolved 24 h in advance in 30 mL Milli-Q water. The experiment lasted 1.5 month and then, measurements below were performed.

Physiological and photosynthesis-related measurements

Photosynthesis parameters Rates of respiration (R), net (P_{net}) and gross (P_{gross}) ($\mu\text{mol O}_2 \text{ h}^{-1}$) photosynthesis were measured for 8 *Stylophora pistillata* and 6 *Turbinaria reniformis* nubbins sampled in the two tanks per condition. Measurements were conducted in Plexiglass chambers (60 ml) filled with 0.45- μm -filtered seawater maintained at the respective experimental temperature (26–32 °C) and continuously homogenized by magnetic stirrers. The oxygen concentration in each chamber was continuously recorded with an optical oxygen sensor (polymer optical fibre, PreSens) connected to an Oxy-4 (channel fibre-optic oxygen metre, PreSens), and processed by the Oxy4v2-30fb software. Calibration was performed at the experimental temperatures (26–32 °C),

at 100% with O₂-saturated seawater and at 0% with seawater saturated with sodium sulfite. P_{net} was monitored at a PAR of 180 μmol photons m⁻² s⁻¹ while respiration rates were subsequently measured in the dark. Nubbins were then frozen at -80 °C to determine symbiont density and chlorophyll *a* and *c*₂ (Chl) content. The single dip wax technique was used to estimate the surface area of the nubbins²³. R, P_{net}, P_{gross}, Chl and symbiont content were normalized to the surface area (cm²).

Pulse-amplitude-modulation fluorometry The relative electron transport rate (rETR) was measured on 8 nubbins of *S. pistillata* and 4 nubbins of *T. reniformis* from each condition using the rapid light curve function of a PAM (Pulse-Amplitude-Modulation) fluorometer (Walz GmbH, Effeltrich, Germany). Briefly 10 min after corals were placed in the dark, the effective quantum yield (ΔF/Fm') and rETR were measured after exposure to ten light intensities for 10-s (10, 17, 26, 41, 74, 130, 220, 664, 1032-μmol·m⁻²·s⁻¹), but we then considered the mean of all rETR values measured at PAR₁₃₀ and PAR₂₂₀, the closest light intensity to which the corals were exposed.

Symbiont density and chlorophyll concentrations The nubbins used for the photosynthesis measurements were thawed and the tissue was separated from the skeleton with the water-pick technique using 9–26 ml of filtered seawater and a Potter tissue grinder. Sub-samples of 50 μL of the extract were used to quantify dinoflagellate density using a LUNA FX7 automated Cell Counter (Logos Biosystems, South Korea). Another sub-sample of 5 ml of the extract was centrifuged at 5530 g for 15 min at 4 °C to separate host tissue and symbionts. Only the fraction (pellet) containing dinoflagellates was kept and resuspended in 5 ml of pure acetone. The resulting solution was kept in the dark at 4 °C during 24 h and then centrifuged for 15 min at 15 °C and 5530 g. The supernatant was read at 750, 663 and 630 nm with a UVmc2 spectrophotometer (Safas). Jeffrey and Humphrey²⁴ equations were employed to calculate chlorophyll *a* and *c*₂ concentration which were then normalized to the skeleton surface area.

Metal analysis in coral tissue

Three nubbins of each species per condition were frozen at -80 °C and further used for metal analysis in the same laboratory as in Blanckaert et al.¹⁶ in the Center for Marine and Environmental Research (Croatia). Tissue was extracted as described in the section above, but in metal free water and with metal free utensils washed with acid (Sigma-Aldrich nitric acid 65% Suprapur[®]) and milli-Q water. Host and symbionts were separated as described above and freeze-dried, and the skeleton was used to measure the surface area as described above. The freeze-dried samples (18.0–53.6 mg of symbionts samples; 4.7–14.4 mg of host samples) were digested in 3 ml concentrated high purity nitric acid (69% HNO₃ ROTIPURAN[®] Supra, Carl Roth) in a microwave oven (Multiwave eco, Anton Paar). Microwave digestion temperature procedure consisted of (1) heating up to 100 °C during 10 min, (2) holding 100 °C for 2 min, (3) increasing temperature to 180 °C during 10 min and (4) holding 180 °C for additional 8 min. Thereafter, 15-mins cooling period is applied. Using the same protocol, procedural/Acid/MilliQ blanks were also determined (*n* = 3). The QC was checked by measuring the element content (*n* = 3) in a certified sample IAEA 461 with relative standard deviation lower than 4% (Trace Elements and Methyl Mercury Mass Fractions in IAEA-461 Clam (*Gafrarium tumidum*) Sample). The recoveries ranged from 77 to 105%. The concentration of metals in the samples was determined as described by Blanckaert et al.¹⁶. The digested samples were diluted to a final volume of 60 mL and used for the determination of the element concentration with the Agilent 8900 ICP-MS-QQQ. Only 10 ppb indium (In) was added to the sample for ICP-MS analysis to serve as an internal standard. Quantification was performed by external calibration with standards (0, 0.1, 1, 10 and 100 ppb) prepared in 2% HNO₃. In addition to a QC sample mentioned above (IAEA 461), a certified standard reference material SLRS-6 (River Water Certified Reference Material for Trace Metals and other Constituents, NRC, Canada) was also used as QC for measurements in low matrix water samples (recoveries obtained were between 98% and 113%). The elements were measured in He and/or H₂ mode. Considering that the digested samples showed no matrix effect after dilution (no change in intensity) and that the recoveries in the certified samples were within the certified values, it is assumed that possible measurement errors are negligible. The process-related blank samples of acidified MilliQ water, which were subjected to the same microwave digestion procedure as the digested samples, did not exceed 10% of the measured concentrations in the majority of samples (98%). The average blank value (*n* = 3) for each metal was subtracted from the samples. The measured concentrations in the samples were at least 10× higher than the detection limit.

Analysis of zinc, copper and iron isotopic composition

The determination of iron, zinc and copper isotopic compositions were carried out according to Maréchal et al.²⁵ and Poitrasson and Freydier²⁶ at the facilities of the Laboratoire Magmas et Volcans (LMV, France). Fully detailed analytical protocol can be found in Sauzéat et al.²⁷. Briefly, after digestion, the samples were evaporated to dryness and the residue was redissolved in a mixture of HCl (8 M) + H₂O₂ (0.001%). Next step consists of isolating and purifying Cu, Fe and Zn by ion-exchange chromatography using 1mL of AG-MP1 anion exchange resin following a revised procedure from Costas-Rodriguez et al.²⁸ and fully described by Sauzéat et al.²⁷. Iron, copper and zinc isotopic compositions were measured using a Thermo Scientific Neptune Plus[™] MC-ICP-MS instrument (LMV, France). Medium mass resolution was used for Cu and Zn isotope ratios while high mass resolution was used for Fe. The overall procedure led to total procedural blanks (*n* = 2) of 9 ng for Cu, 8 ng for Zn and around 10 ng for Fe, which represents less than 1% of the amount of each element present in the sample solutions. The long-term precision of the results was assessed by sample re-run analysis and repeated measurements of the bracketing standards run every two samples. Sample accuracy was assessed by the measurement of certified biological reference material (bovine liver 1577c). The long-term external standard reproducibility (2sd) was better than 0.1‰ (*n* = 20) and our results of the certified reference 1577c material are in good agreement (±0.06‰ (2sd,

$n=6$) with certified values for all isotope ratio measurements (see Supplementary Table S8 online). Given our long-term precision and the accuracy obtained on reference material measurements, the two-standard deviation (2sd) analytical uncertainty adopted in this study for the Cu, Zn and Fe isotopic compositions is $\pm 0.06\%$.

Antioxidant and oxidative stress markers

We used the same nubbins for all antioxidant and oxidative stress marker reactions, i.e. 3–5 nubbins of *S. pistillata* and 1–2 nubbins of *T. reiniformis* per condition. However, the number of replicates varies between the stress markers as the measurements did not work for every nubbin. Therefore, several measurements of oxidative stress are only informative. Lipid peroxidation (LPO) was quantified by measuring the levels of thiobarbituric acid reactive substances (TBARS), according to Oakes and van der Kraak²⁹. Samples were added to 200 μL of KCl solution (1.15%) containing 35 μM butylatedhydroxytoluene (BHT), sonicated (20 pulses at 70%, Vibra-CellTM; Bioblock Scientific) and centrifuged (11000 RPM, 4 °C) for 10 min. Supernatant was transferred to new tubes and centrifuged again. Bradford protein assay³⁰ of *S. pistillata* was conducted by adding triplicates of 5 μL of each sample in a microplate and 250 μL of Coomassie reagent in each locus. While Bradford protein assay of *T. reiniformis* was conducted by adding triplicates of 25 μL of each sample in a microplate and 225 μL of Coomassie reagent in each locus. The plates were read at 595 nm. Samples were then standardized to 280.9 μg . μL^{-1} . Standards were made with tetramethoxypropane (TMP) hydrolysed into MDA. 150 μL of acetic acid solution (20%), 150 μL of TBA solution (0.8%), 50 μL of MilliQ and 20 μL of sodium dodecyl sulfate solution (8.1%) were added to each sample and standard, vortexed and then incubated for 30 min at 95 °C. The tubes were cooled down for 10 min in the dark, then added to 100 μL of MilliQ water and 500 μL n-butanol, vortexed and centrifuged for 10 min at 3000 rpm (15 °C). 150 μL of the supernatant (organic phase) were added in 96-well black plate in duplicates and the fluorescence was read at 515 and 553 nm under a frequency of 1 min^{-1} for 3 min (Xenius[®], SAFAS, Monaco). Results are expressed in thiobarbituric acid reactive substances (TBARS) (nmol mg protein⁻¹).

Total antioxidant capacity (TAC) essays were conducted using the OxiSelect TAC Assay Kit (STA- 360, Cell Biolabs Inc.) according to the manufacturer's instructions. Bradford protein assay was conducted as described above, except that the homogenization solution used was PBS (pH 7.4). Samples were then standardized to 278.9 μg . μL^{-1} . More details can be found in Blanckaert et al.¹⁶

Catalase activity was measured using the Calorimetric Activity Kit (EIACATC, Thermo Fisher Scientific) while the activity of glutathione peroxidase was measured using the Glutathione Peroxidase Assay Kit (MAK437, Sigma-Aldrich) according to the manufacturer's instructions with at least 2 nubbins of *S. pistillata* and *T. reiniformis* per conditions previously kept at 80 °C. Bradford protein assay was conducted as described above, except that the homogenization solution used was PBS (pH 7.4) and centrifugation was at 10,000 G for 10 min at 4 °C. Samples were then standardized to 0.9 μg . μL^{-1} . Normalization was done using the total protein contained in the 1 cm nubbin.

Statistical analysis

The effects of temperature and dust on coral physiology and metal content were assessed using two-way ANOVA and pair-wise Tukey HSD (honestly significant difference) tests, considering each normalized ecophysiological measurement (P_{gross} , P_{net} , Chl, symbionts densities and mean rETR PAR₁₃₀-PAR₂₂₀) and the metal content in the tissues (Li, Mg, V, Cr, Mn, Fe, Co, Ni, Cu, Zn, As, Mo, Cd) as dependent variables and temperature and dust conditions as interacting factors. Data were log, square root or boxcox transformed to achieve ANOVA assumptions, which were tested with Levene's and Shapiro-Wilk tests. When homoscedasticity was not reached, a Wilcoxon rank sum test (Benjamini-Hochberg) was conducted. The significance level adopted was $p \leq 0.05$, although the significance of $p < 0.1$ was not discarded and will be specifically mentioned in the result table. Only the results for which dust or the interaction between dust and temperature which significantly affected the metallome of the symbionts or host tissues will be presented. Few results, which were not significantly different between treatments, are still presented in the result section as they are visually showing trends, but this information will be specified in figures and tables.

To understand how the dust-induced changes in the metallome of corals explain the variability in coral physiological proxies, redundancy analyses (RDA)^{31,32} were performed. These analyses included only response variables which changed with treatments, and explanatory variables that were significantly ($p < 0.1$) or visually affected by dust. A variable was considered visually affected by dust when the results of two-way ANOVA were not significant, but a systematic trend of dust effect was observed at both temperatures (e.g. Fig. 4 - Ni and Cr). Those criteria were chosen to exclude response variables that did not react to the experimental conditions, and to focus on explanatory variables influenced by dust. This focus is essential because RDA can only accommodate a limited number of explanatory variables. Scaled P_{net} , rETR, symbionts density, chlorophyll a and c2 concentrations, catalase activity, TAC (only in *S. pistillata*) and glutathione activity (only in *S. pistillata*) were the used response variables. As the rETR, the oxidative stress markers and the metals content were measured in nubbins different than those of the other photosynthetic proxies, we than averaged those values for the corresponded aquaria. Metals content that were significantly or visually affected by dust provision (Li_{sym} , Mg_{sym} , Mn_{sym} , Fe_{sym} , Mo_{sym} , Ni_{sym} , Cr_{host} , Fe_{host} , Mn_{host} and Mo_{host} in *S. pistillata*, and Mg_{sym} , Li_{sym} , Ni_{sym} , Cr_{sym} , Cu_{host} , Zn_{host} , Ni_{host} and Cd_{host} in *T. reiniformis*) and that did not have a high leverage outlier (e.g. Cr_{sym} in *S. pistillata*), were initially considered as explanatory variables. Due to the high collinearity ($R^2 > 0.9$), the scaled Li, Fe & Mn of the symbionts of *S. pistillata* were averaged and analyzed together as a single composite variable ($\text{Fe Li \& Mn}_{\text{sym}}$). Because the number of explanatory variables was still high, we reduced it by using the R adjusted forward stepwise selection (999 permutations) ($p < 0.1$). We finally run another RDA only with the significant explanatory variables and tested for variance inflation factor (VIF) ≤ 10 . We also present ANOVA permutation tests for Redundancy Analysis (RDA). The results are displayed in an RDA biplot for each species separately.

All statistical tests and produced images were processed in the Rstudio 2023.12.1 + 402 software. Stable isotopic composition was added as additional explanatory variables in RDA biplots displayed in the supplementary material, as VIF values are ≤ 21 . The interquartile of boxplots ranged from 25th to 75th percentile, and whiskers point to the largest value within 1.5 times interquartile range above 75th percentile or the smallest value within 1.5 times interquartile range above 25th percentile. The final layout of all figures was done in Inkscape 1.1.2, www.inkscape.org.

Iron experiment

Since dust releases high amounts of iron in seawater, which could have triggered the observed photophysiological changes in the corals, we tested whether an increased supply of iron, either in the form of ferric chloride or ferric citrate, would improve the photosynthetic performance of the symbionts. For each treatment, three nubbins from three different colonies were placed in individual 400 mL beakers for 6 h each day, and returned to two mother aquaria overnight. The corals were exposed to iron enrichment, at 26 °C and 200 $\mu\text{mol photon m}^{-2} \text{s}^{-1}$ for three weeks.

To enrich seawater with iron, 50 μL spikes containing 8 nM of iron chloride (dissolved in MilliQ water), or 8 nM of ferric citrate (dissolved in MilliQ water) or simply MilliQ water (control) were added to triplicated beakers, at the beginning of the exposure, and again 3 h later, so that 20 nM iron was added to each beaker in the morning, and another 20 nM in the afternoon. The addition of 40 nM per day is equivalent to the highest amount of iron added by dust (approx. 52 nM) compared to the mean quantity of iron detected in the control water (approx. 13 nM) in Blanckaert et al. 2022. At the end of the exposure, the nubbins were washed three times in clean filtered seawater to remove all metal residues in the mucus. The rates of photosynthesis and electron transport (rETR) were measured at the end as described in the chapters above. Four nubbins were selected to conduct the photosynthesis measurements, and six nubbins were selected for conducting the relative electron transport rate measurements. After 3 weeks, the temperature was increased by 0.5 °C per day, and the photosynthesis and electron transport rate measurements were performed again as described above three weeks after the start of heating.

Results

Physiological and photosynthesis-related responses to temperature and dust conditions

Dust provision, high temperature or a combination of both factors had significant effects on the photophysiological parameters of *S. pistillata*. The detailed effects of each experimental condition are complex and are summarized in Table 1 and presented in Fig. 1a – e. No significant difference in photophysiological parameters was observed in corals maintained at the control temperature of 26 °C with or without dust, suggesting that dust provision at a normal growth temperature did not improve the photophysiology of *S. pistillata*. The most significant effects were observed between heat-stressed corals without dust provision (32 °C-Ø) and the other treatments. P_{gross} and symbiont density decreased significantly at 32 °C-Ø compared to the control condition of 26 °C-Ø, showing a certain degree of heat stress in corals at high temperature. In addition, P_{gross} , symbiont and chlorophyll density were significantly lower at 32 °C-Ø compared to 32 °C-dust, the latter condition being not different from the control condition. Finally, P_{net} , P_{gross} , symbiont density and rETR ($\text{PAR}_{130} - \text{PAR}_{220}$) were significantly lower under 32 °C-Ø than under 26 °C-dust, suggesting that the best conditions for the photosynthetic machinery of *S. pistillata* were achieved under normal growth temperature and dust provision.

Slightly different from *S. pistillata*, dust provision and high temperature have an independent effect on the physiological parameters of *T. reniformis* (see Supplementary Table S1 online, Fig. 2a – e). The detailed effects on each experimental condition are shown in Table 1; Fig. 2. Overall, under the normal temperature conditions (26 °C), only chlorophyll content was significantly increased by dust provision (Fig. 2d), although the other

<i>Stylophora pistillata</i>					
Photophysiology	Dust signif.	Temperature signif.	Interaction signif.	Dust addition at 26°C	Dust addition at 32°C
P_{gross}	<0.05	<0.05	<0.05	=	↑
P_{net}	<0.05	<0.05	<0.05	↑	↑
Symbionts density	<0.05	<0.05	<0.05	=	↑
Chlorophyll density			<0.05	=	↑
ETR $\text{PAR}_{130} - \text{PAR}_{220}$	<0.05			↑	=
<i>Turbinaria reniformis</i>					
P_{gross}	<0.05	<0.05		=	↑
P_{net}	<0.05	<0.05		↑	↑
Symbionts density	<0.05	<0.05		↑	↑
Chlorophyll density	<0.05	<0.05		↑	↑
ETR $\text{PAR}_{130} - \text{PAR}_{220}$	<0.1	<0.05		↑	↑

Table 1. Table summarizing the effects of dust, temperature, and their interaction on the above photophysiological parameters measured in *S. pistillata* and *T. reniformis* (see Supplementary Table S1 online). Visual changes that were not confirmed by the Tukey test are marked with a dashed arrow (see Supplementary Table S1 online).

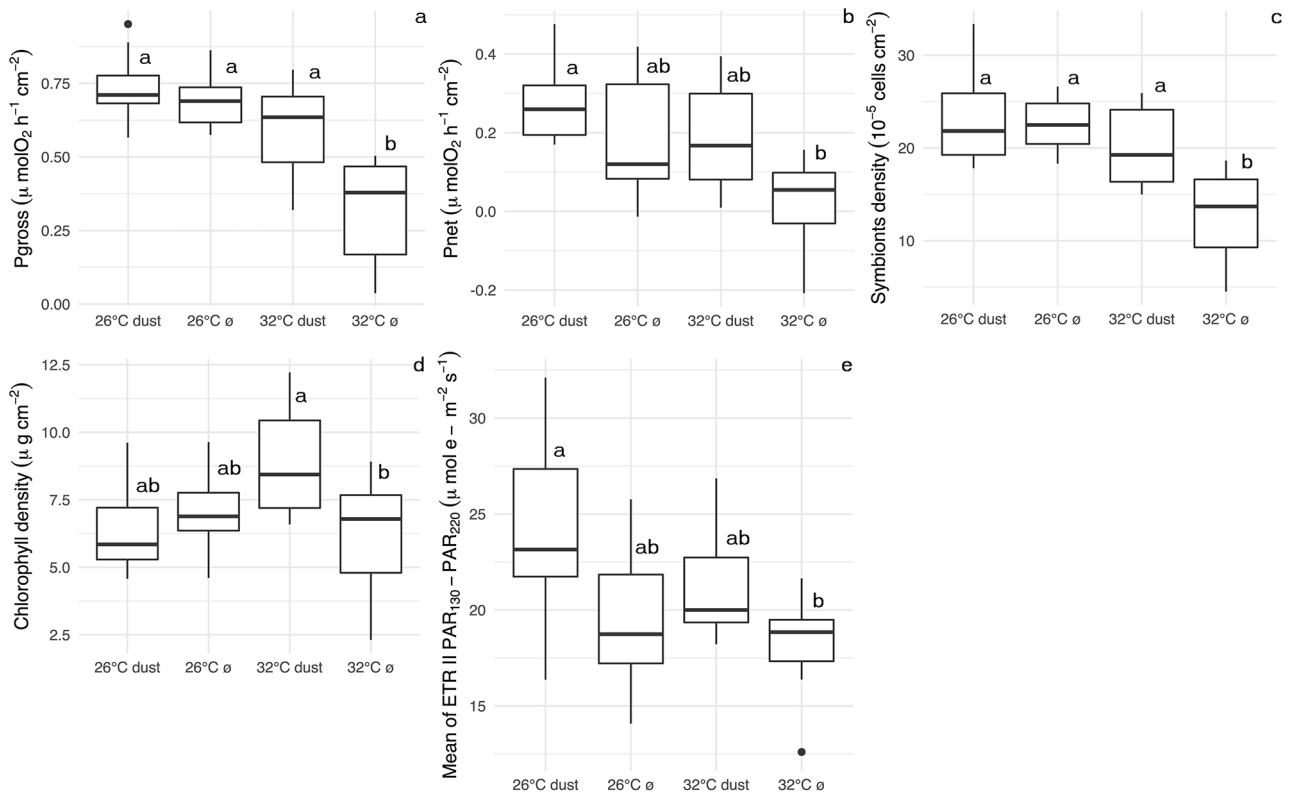


Fig. 1. Physiological and photosynthesis-related measurements in *S. pistillata*. Gross (a) and net photosynthesis (b), symbionts density (c), chlorophyll content (d) and electron transport rate at PAR₁₃₀-PAR₂₂₀ (rETR) in *S. pistillata*.

photophysiological parameters, such as P_{gross} , P_{net} and symbiont density, tended to be higher under dust supply condition. Similar to *S. pistillata*, the photophysiological parameters of the heat-stressed corals under dust provision (32 °C-dust) were not significantly different from those of the control corals (26 °C-Ø), while the heat-stressed corals without dust significantly decreased their P_{gross} , P_{net} and symbiont density compared to the control (Fig. 2, abd). Moreover, similar to *S. pistillata*, all parameters (P_{net} , P_{gross} , symbiont density, chlorophyll content and rETR) were significantly lower at 32 °C-Ø than at 26 °C-dust, suggesting that the best conditions for the photosynthetic machinery of *T. reniformis* were achieved at normal growth temperature and dust provision.

Oxidative stress markers

The antioxidant responses, assessed by three complementary methods including the total antioxidant capacity (TAC), glutathione peroxidase (GPX) and catalase activities, showed clearer trends in *S. pistillata* than in *T. reniformis* and were different in dust-treated and control corals (Fig. 3). While TAC was significantly higher in the dust-treated *S. pistillata* (see Supplementary table S1 online), catalase and GPX activities tended to be higher in the non-dust corals. *T. reniformis* showed no clear changes in TAC as a function of temperature or dust provision, while catalase activity was activated by dust only at 32 °C condition. Lipid peroxidation did not change in either coral species under all conditions (see Supplementary Fig. S2 online). Note that the Total Antioxidant Capacity (TAC) assay measures the total antioxidant capacity of biomolecules based on reduction of copper (II) to copper(I), with a preferential efficiency for low molecular molecules (e.g., thiols) compared to GPX and CAT, which might explain the results discrepancies (Fig. 3).

Metal content

The results show significant effects of dust and temperature on the metallome of both the host tissue and the symbionts of *S. pistillata* and *T. reniformis*, with greater effects in *S. pistillata* (Figs. 4, 5, 6 and 7; Table 2; see Supplementary Table S1 online). Dust provision significantly increased the metal content of *S. pistillata* symbionts (Li, Mg, Mn, Fe, Cr, Mo (at 32 °C)), and to a lesser extent, that of *T. reniformis* symbionts (Li and Mg). Dust provision also increased the metal content of *S. pistillata* host (Cr, Mn, Fe and Mo). Under dust provision, certain metals were present in lower concentrations in the symbionts (Ni, Co, Cr) and the host (Ni, Cd, Cu, Zn) of *T. reniformis*, as was Ni in the symbionts of *S. pistillata*.

Some metals were also affected by temperature alone, but differently depending on species, and host or symbiont compartments (see Supplementary Table S1; Supplementary Fig. S3 – S6 online). In *T. reniformis*, Fe increased with temperature in the symbionts and host, as well as Cr ($p < 0.1$) in the host, while As was decreased

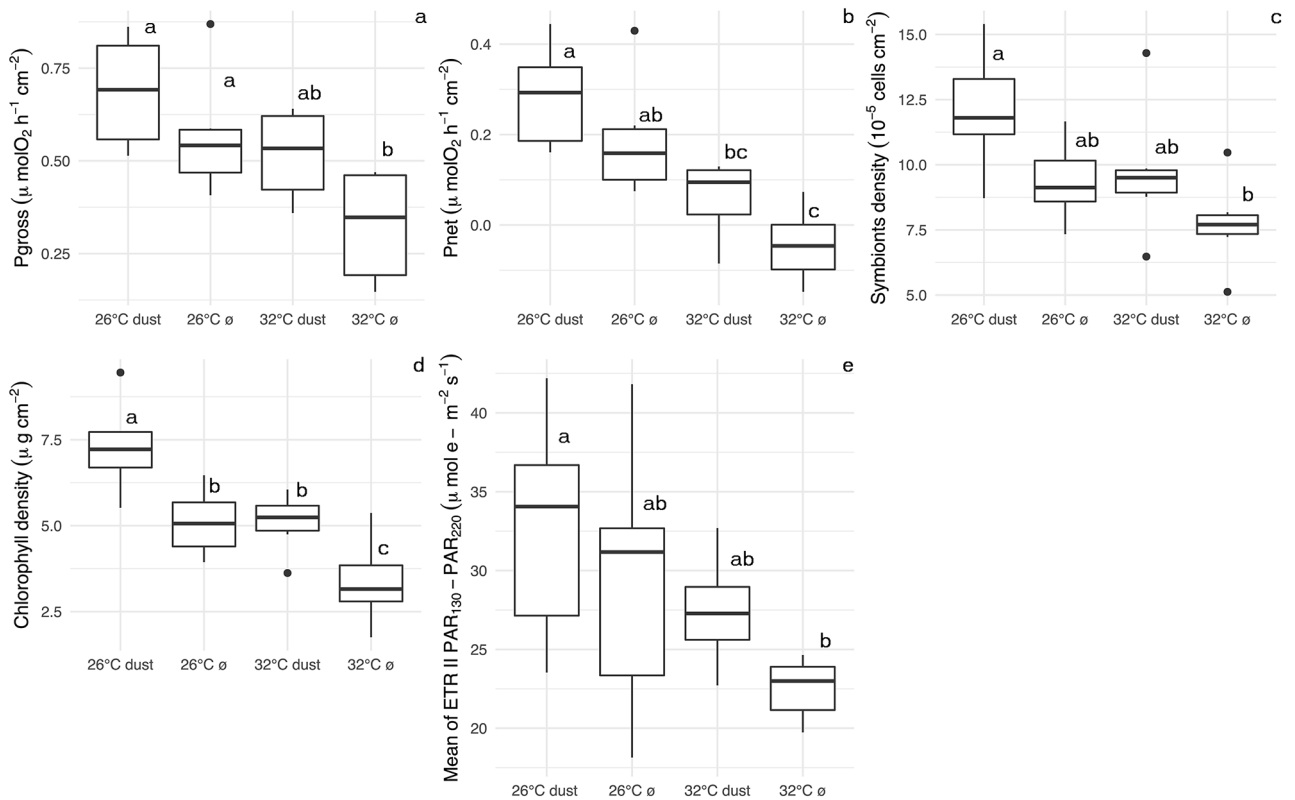


Fig. 2. Physiological and photosynthesis-related measurements in *T. reniformis*. Gross (a) and net photosynthesis (b), symbionts density (c), chlorophyll content (d) and electron transport rate at PAR₁₃₀–PAR₂₂₀ (rETR) (e) in *T. reniformis*.

in the symbionts. In *S. pistillata*, Cr and Ni were enhanced by temperature in the symbionts and Li and Mg in the host. However, As and Cd ($p < 0.1$) decreased with temperature in the symbionts and V, Zn and Cd in the host.

To further explore how the changes in host and symbiont metallome are linked to the changes in coral photophysiology, we ran redundancy analyses (RDA) ordination models in a following section.

$\delta^{66}\text{Zn}$, $\delta^{56}\text{Fe}$ and $\delta^{65}\text{Cu}$ bulk stable isotope analysis

Copper ($\delta^{65}\text{Cu}$), zinc ($\delta^{66}\text{Zn}$) and iron ($\delta^{56}\text{Fe}$) isotopic values are function of the coral species, temperature and dust provision, and the intensity of the isotopic fractionations were compartment-dependent (i.e., host tissues vs. symbionts) (Fig. 8).

$\delta^{56}\text{Fe}$ was enriched in almost all dust-treated samples compared to the non-dust conditions at both 26 °C and 32 °C. Dust-treated symbionts of *T. reniformis* were depleted in $\delta^{66}\text{Zn}$ values whereas symbionts of *S. pistillata* were enriched in $\delta^{66}\text{Zn}$ values. Under control conditions (no dust) $\delta^{66}\text{Zn}$ and $\delta^{65}\text{Cu}$, in both symbionts and host tissues of *S. pistillata* increased with temperature. This T°C-dependent increase extend to $\delta^{56}\text{Fe}$ in *T. reniformis*. Under dust provision conditions, $\delta^{66}\text{Zn}$ tend to globally be higher at 26 °C than at 32 °C. In average, similar variations were observed for $\delta^{65}\text{Cu}$ except for *S. pistillata* symbionts for which $\delta^{65}\text{Cu}$ rise from +0.56 to +0.86‰ at 32 °C.

Link between the changes in metallome and physiology under dust provision

The first and second ordination axes of the RDA model explained 47% and 29% of the photophysiological variation in *S. pistillata* respectively, while the first and second axes explained 78% and 13% in *T. reniformis*, respectively (Fig. 9). The results of the marginal ANOVA performed with the RDA models showed significant effects of all added metals on the physiological traits of both corals (see Supplementary Table S8 online). More specifically, Fe, Mn & Li_{sym} composite vector was positively related to the chlorophyll a content in samples of *S. pistillata*, while Mg_{sym} and Mo_{sym} were slightly related to both chlorophyll a and c2 in *S. pistillata*, especially in samples maintained at 32 °C-dust. The Li_{sym} was also positively related to the photosynthesis of *T. reniformis*. The catalase (Cat) and glutathione peroxidase (GPX) activities tended to be opposite to all photophysiological proxies. TAC tended to be higher at the 32 °C-dust.

Metals which were decreased by dust (Ni_{sym} in *S. pistillata* and Co_{sym}, Ni_{sym} and Cu_{host} in *T. reniformis*) were anti-correlated to the photophysiological parameters in both species, except Co_{sym} and Cu_{host} in *T. reniformis* which did not have any clear relation to photosynthesis.

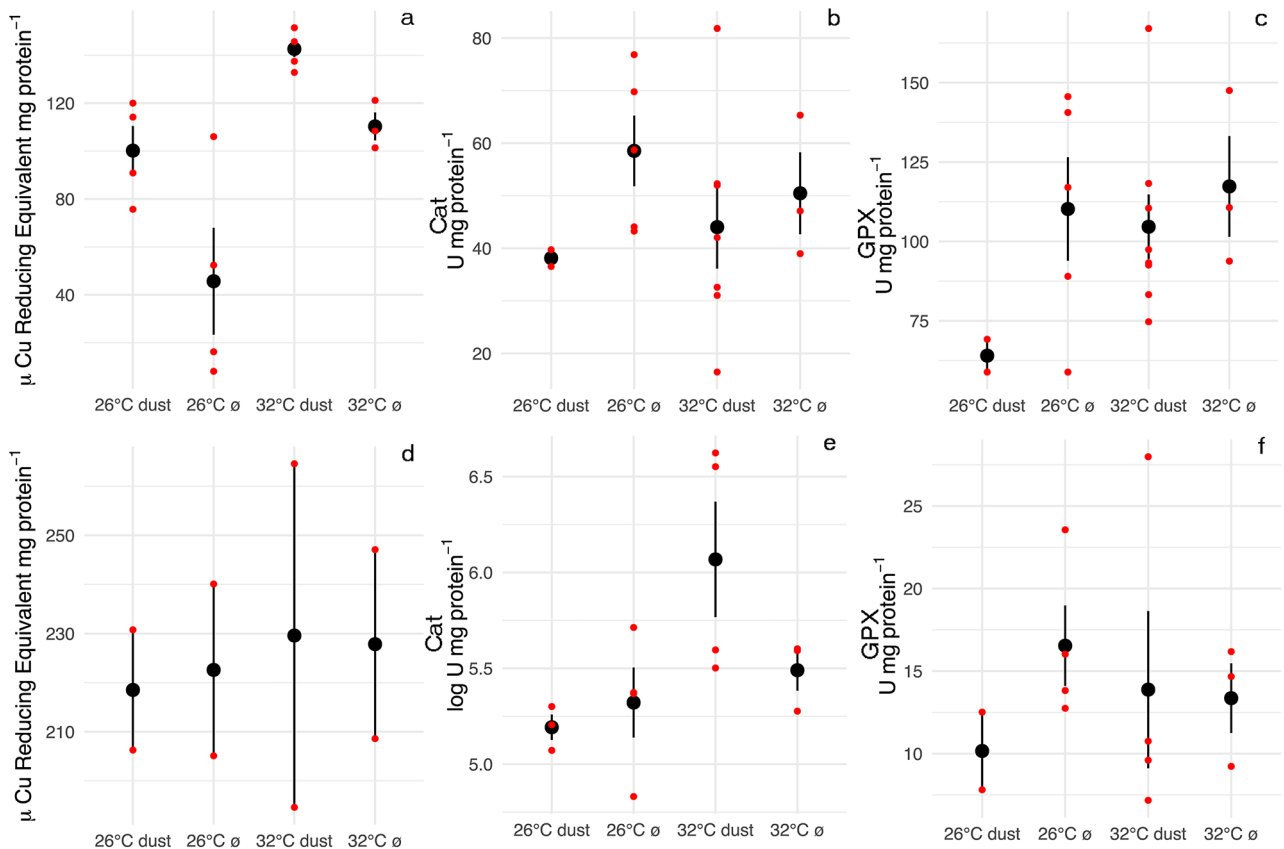


Fig. 3. Antioxidant and oxidative stress markers. Total antioxidant capacity (TAC) (μM Cu reducing equivalents $^{-1}$), catalase (U mg protein $^{-1}$) and glutathione peroxidase (GPX) (U mg protein $^{-1}$) activities in *S. pistillata* (TAC - **a**; Catalase - **b**; GPX - **c**) and in *T. reiniformis* (TAC - **d**; Catalase - **e**; GPX - **f**).

Iron experiment

No significant effect of iron (both ferric chloride and ferric citrate) was found before or after thermal stress (Fig. 10) on the P_{net} and P_{gross} of *S. pistillata*. rETR was slightly negatively affected by iron provision ($p \leq 0.1$). P_{net} and P_{gross} were significantly decreased by heat stress only (see Supplementary Table S1 online).

Discussion

Desert dust is considered an important nutrient source for marine primary productivity¹⁹. Dust storms could thus be particularly important in environments surrounded by deserts and characterized by nutrient scarcity, such as the northern Red Sea. In this context, the present study investigated the effects of desert dust provision on the photophysiological response and metallome of the symbionts and host of two Red Sea scleractinian corals (*Stylophora pistillata* and *Turbinaria reiniformis*) exposed to thermal stress. The main finding is that dust provision enhanced the photophysiological functions of corals during heat stress and enriched the coral hosts and symbionts with several metals (e.g.: Li, Mn, Fe, Mg, Mo), especially in *S. pistillata*. Our results obtained in restricted conditions (only Fe supplementation) indicate that iron supply is not the direct promoter of the observed increase in photosynthesis under dust provision. Furthermore, we found that dust plays an important role in reducing the uptake of metals such as Ni, which is here negatively related to photosynthesis. Ni is usually taken up by corals to transform urea into inorganic nitrogen under nitrogen deficiency. Finally, we observed the dust provided the coral symbionts with Li, a trace element that exhibits both toxic and beneficial properties in trace amounts. However, the exact functions of each of these ions require further research.

Species-specific effects of dust supplementation on the metallome and physiology of corals

In both coral species, the dust-derived metals accumulated mainly in the Symbiodiniaceae as previously observed^{10,16,17}. Symbionts indeed have a high demand in several metals such as Fe, Mg, Mn, Zn, which are essential for all steps of the photosynthetic process¹², as well as in the composition of antioxidant enzymes produced under stress conditions^{32–36}.

The effects of dust provision were however species (or holobiont)-specific, since the two scleractinian coral species altered their metallome differently in response to dust provision. While the symbionts of *S. pistillata* were enriched in a variety of metals such as Li, Mg, Mn, Mo, Fe and Cr when supplied with dust (either at 26–32 °C), the symbionts of *T. reiniformis* accumulated mainly Li and Mg. The same could be observed in the host tissue, as *S. pistillata* accumulated more metals (Mn, Mo, Fe and Cr) than *T. reiniformis* (Cd at 32 °C). This difference

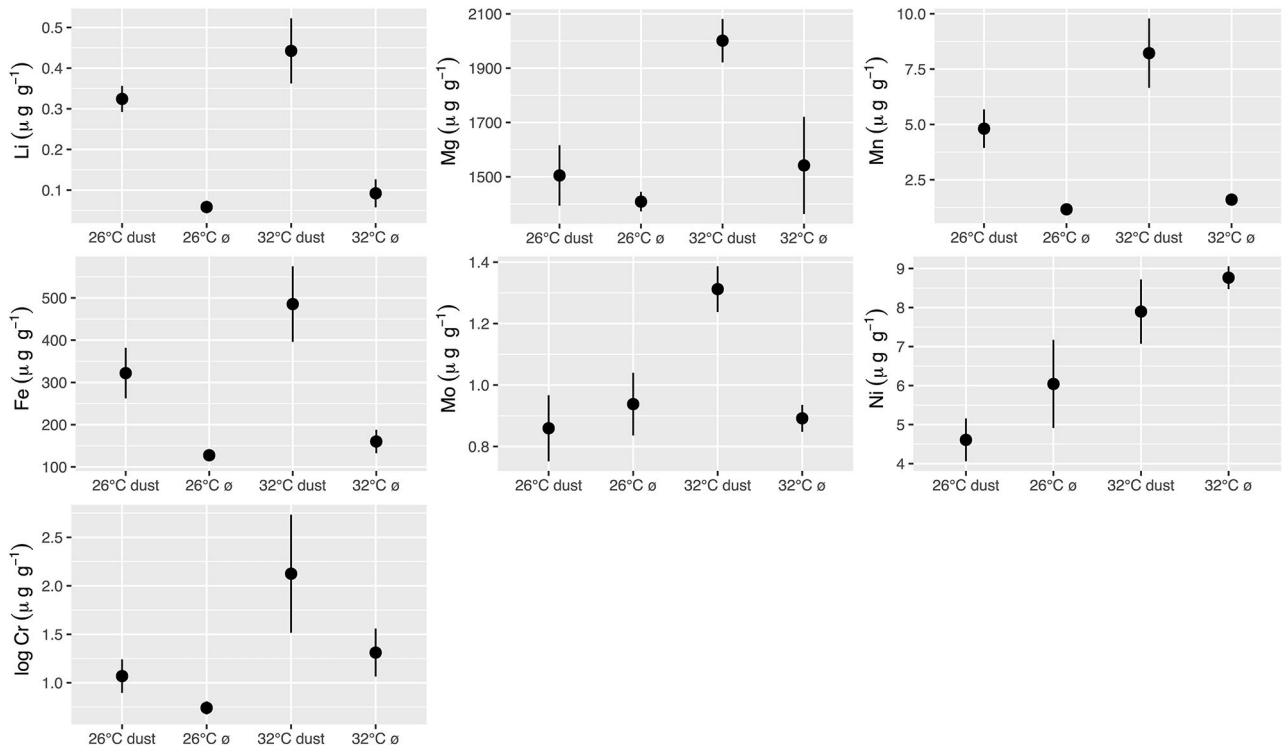


Fig. 4. Metals content in the symbionts of *S. pistillata*. Mean ($n=3$) and standard deviation of the content of Li, Mg, Mn, Fe, Mo, Ni and Cr in the symbionts of *S. pistillata*. Effect of dust on Mo was significant with $p < 0.1$, and Ni and Cr did not show significant differences with dust or with the interaction between dust and temperature, but we still will refer them as influenced by dust based on visual trend (Table 2).

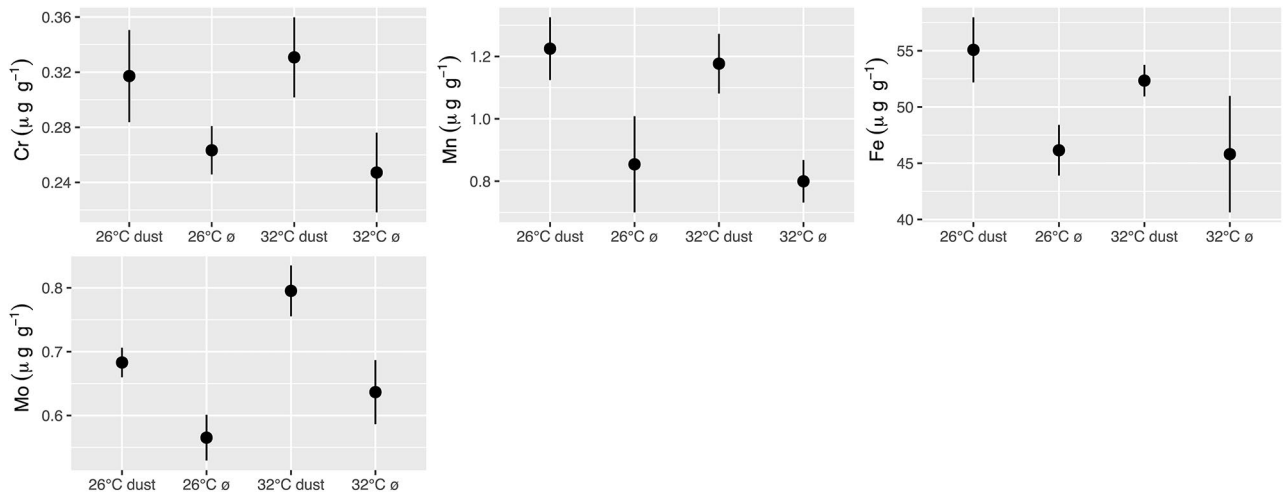


Fig. 5. Metals content in the host of *S. pistillata*. Mean ($n=3$) and standard deviation of the content of Cr, Mn, Fe, Mo in the host of *S. pistillata* (Table 2).

may be due to holobiont-specific requirements for metals or capacities to take up metals from seawater. For example, the Symbiodiniaceae genotype hosted by the two species are different, Clade A in *S. pistillata*^{37–39} and Clade C in *T. reniformis*⁴⁰ may have different metal requirements¹². Alternatively, different coral species may have a different allocation of dust-derived metals between host and symbionts which cannot be assessed by measuring metal concentrations alone. Due to the relatively lower biomass of the symbiont compartment compared to the host compartment, the metals taken up by the corals supplied with dust tend to be more concentrated in the symbionts. Therefore, it is more likely that changes in metal concentration will be observed in the symbionts than in the host compartment. In other words, the absence of a change in metal concentration in the host compartment does not necessarily mean that the metals were not supplied in larger quantities under

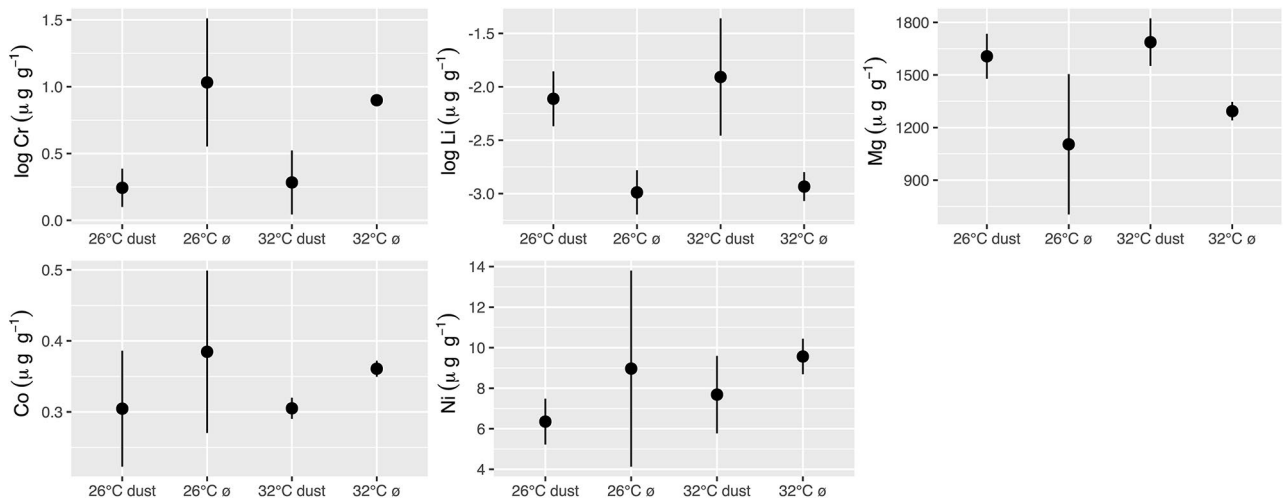


Fig. 6. Metals content in the symbionts of *T. reniformis*. Mean ($n=3$) and standard deviation of the content of Cr, Li, Mg, Co and Ni in the symbionts of *T. reniformis*. Effect of dust on Mg was significant at $p < 0.1$, and Ni and Co did not show significant differences with dust or with the interaction between dust and temperature, but we still will refer them as influenced by dust based on visual trend (Table 2).

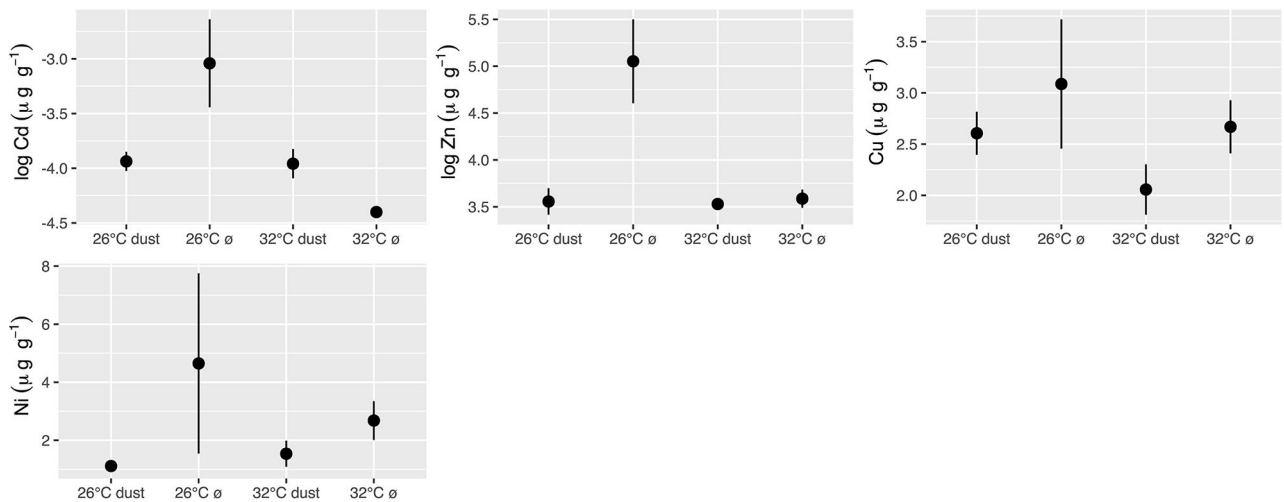


Fig. 7. Metals content in the host of *T. reniformis*. Mean ($n=3$) and standard deviation of the content of Cd, Zn, Cu and Ni in the host of *T. reniformis*. Ni and Cu did not show significant differences with dust or with the interaction between dust and temperature, but we still will refer them as influenced by dust based on visual trend (Table 2).

dust provision. This challenge can be addressed by a combined analysis of metal concentration and metal stable isotopic compositions.

The isotopic measurements showed a consistent enrichment of $d^{56}\text{Fe}$ in the symbionts and host of *T. reniformis* and *S. pistillata* supplied with dust. This $d^{56}\text{Fe}$ enrichment might be the sign of direct Fe-rich dust contamination but the similar Fe isotopic values of dust and seawater (0.1‰ for dust⁴¹ and 0.0–0.5‰ for surface non-edge affected for seawater⁴²) does not point toward this hypothesis, unless chemical/physical processes induced by dust dissolution have fractionated iron, for instance by addition of silicates, carbonates, organic ligands, etc⁴³. Many of these processes can fractionate iron isotopes to different extents and can result in a shift in the $\delta^{56}\text{Fe}$ values in corals. For example, under oxygen-rich conditions like during photosynthesis, preferential uptake of heavier iron can also be favored due to Fe oxidation in the medium. Enrichment of $d^{56}\text{Fe}$ was previously observed in eucaryotic phytoplankton cells⁴⁴, in the surface of cyanobacteria^{45,46} and other microorganism cells⁴³ compared to their medium. These studies suggested that heavy iron isotope signatures resulted from Fe²⁺ oxidation into Fe³⁺ due to photosynthetic derived oxygen^{44,46}. However, this is unlikely in our study, as the Pnet is higher at 26 °C compared to 32 °C condition (Figs. 1b and 2b), while $d^{56}\text{Fe}$ is lighter at 26 °C compared to 32 °C condition (Fig. 8). Other physico-chemical processes induced by dust dissolution, as well as biological processes like the ones regulating metal uptake and internal homeostasis could also have affected the $d^{56}\text{Fe}$ in coral tissue.

<i>Stylophora pistillata</i>					
Symbionts					
Metals	Dust signif.	Temperature signif.	Interaction signif.	Dust addition at 26°C	Dust addition at 32°C
Li	<0.05			↑	↑
Mg	<0.05	<0.05		↑	↑
Mn	<0.05	<0.1		↑	↑
Fe	<0.05			↑	↑
Mo	<0.1	<0.05	<0.05	=	↑
Cr	visual trend	<0.05		↑	↑
Ni	visual trend	<0.05		↓	↓
Host					
Cr	<0.05			↑	↑
Mn	<0.05			↑	↑
Fe	<0.05			↑	↑
Mo	<0.05	<0.05		↑	↑
<i>Turbinaria reniformis</i>					
Symbionts					
Li	<0.05			↑	↑
Mg	<0.1			↑	↑
Cr	<0.05			↓	↓
Co	visual trend			↓	↓
Ni	visual trend	<0.05		↓	↓
Host					
Cd		<0.05	<0.05	↓	↑
Zn	<0.05	<0.05	<0.05	↓	=
Cu	visual trend			↓	↓
Ni	visual trend			↓	↓

Table 2. Table summarizing the effects of dust, temperature and their interaction on the metal content of the host tissue or symbionts of *S. pistillata* and *T. reniformis*. Colored cells are indications of increased (blue) or decreased (orange) metal content in the symbionts or host tissue of both species under dust provision (Figs. 4, 5, 6 and 7). Visual decreases or increases that were not confirmed by the Tukey test are marked with a dashed arrow (see Supplementary Table S1 online).

Altered oxidative stress conditions can also affect redox-sensitive isotopic ratio and might partially explain the higher $d^{56}\text{Fe}$ in dust exposed corals as suggested by similar TAC (Fig. 3) and $d^{56}\text{Fe}$ (Fig. 8, see Supplementary Fig. S12 online) variations for *S. pistillata* under dust conditions. Further studies must be carried out to precisely define mechanisms governing Fe uptake mechanisms and isotope fractionation in corals. This is important as Fe isotopic composition is not only higher in dust-enriched corals, but also in heterotrophically fed corals¹⁴ and heat-stress corals (this study) and seems therefore to be a good proxy for both temperature and feeding conditions.

We also observed changes in Zn and Cu isotopic values following dust provision in *T. reniformis* and *S. pistillata* (Fig. 8). However, the changes were not consistent between coral species. For example, *T. reniformis* showed depleted values of $d^{66}\text{Zn}$ upon dust provision, as would be expected for most primary producers^{47,48} considering that the Saharan dust has a lighter Zn isotopic composition (0.19‰)⁴⁹ compared to the Indian and Atlantic oceans (0.69–1.00‰)⁵⁰. In contrast, *S. pistillata* showed enriched values in both host and symbionts, as if Zn was bound to organic ligands before being taken up by the coral. Such contradictory fractionation of Zn has previously been observed with different strains of cyanobacteria⁴⁸. As organic ligands tend to form complexes with heavy zinc^{51–54}, we assume that the observed enrichment was due to uptake of complexed Zn ligands by *S. pistillata*. Comparable to $d^{66}\text{Zn}$, under dust exposure $d^{65}\text{Cu}$ increased in host and symbionts of *S. pistillata* at 32 °C but decreased in *T. reniformis* (Fig. 8) confirming that each coral holobiont respond differently to dust exposure depending on its physiological needs. Like for $d^{56}\text{Fe}$, further studies need to be conducted to fully understand the observed changes in Cu and Zn isotopic variations in both coral species.

In contrast to the previous metals, Li was one of the metals that consistently accumulated in the symbionts of both coral species supplied with dust and was positively related to coral photophysiology, suggesting that its uptake into the symbionts was related to their photosynthesis activity. Li is a metal naturally present in seawater and derived from terrestrial mineral weathering and basalt-hydrothermal fluxes⁵⁵, with markedly high Li concentrations found at the surface waters of desert dust deposition zones⁵⁶. Li is incorporated in the aragonite

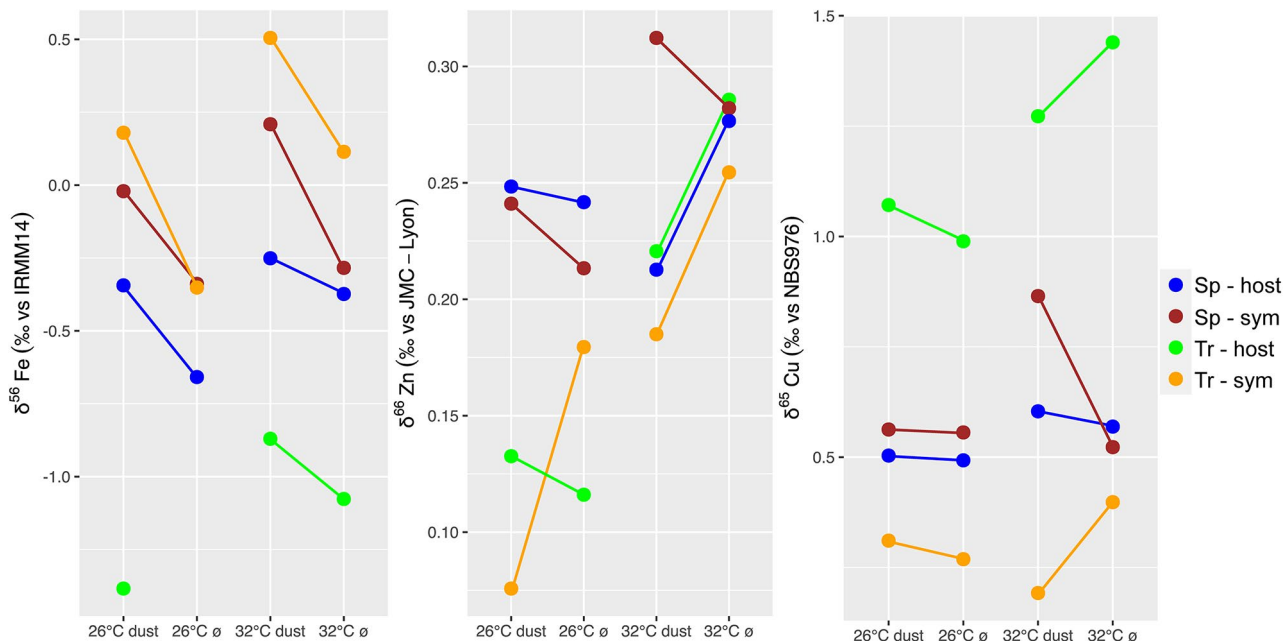


Fig. 8. Iron, zinc and copper isotopic composition. Dust and temperature-dependent variations of $\delta^{56}\text{Fe}_{\text{IRMM14}}$, $\delta^{66}\text{Zn}_{\text{JMC-Lyon}}$ and $\delta^{65}\text{Cu}_{\text{NBS976}}$ in symbionts (sym) and host tissue (host) of *S. pistillata* (Sp) and *T. reiniformis* (Tr).

skeleton of corals⁵⁷, with different isotopic composition between symbiotic (zooxanthellate) and asymbiotic (azooxanthellate) corals⁵⁷, suggesting an involvement of symbionts in Li uptake. In addition, a recent review, describing Li proteome, transcriptome, and metabolome highlighted the role of Li for some gene expression, mitochondrial function, and its influence on other cellular processes such as cell proliferation⁵⁸.

Finally, the Ni content in corals was reduced by dust addition and was negatively related to the photophysiological proxies. When phytoplankton and coral symbionts are limited in ammonium and nitrate, Ni is required for the synthesis of urease, an enzyme needed for the hydrolysis of urea into carbon dioxide and ammonia^{59–61}. The lower Ni uptake in dust-treated corals may be explained by a greater reliance of coral symbionts on other nitrogen sources for their growth. This is in agreement with the fact that dust releases low amount of nitrate in seawater¹⁶, which may replace urea for the nitrogen requirements of symbionts.

The supply of dust helped to maintain a functional symbiosis in both species under thermal stress. A significant decrease in at least one photosynthesis-related variable was observed in colonies exposed to heat stress and not receiving dust. Similarly, under 25 °C condition, a beneficial effect of metal supplementation was observed in corals supplied either with desert dust¹⁶ or volcanic ash¹⁷. In addition, the results of this study show that PSII of dust-treated nubbins performed better at 26 °C than in the other treatments, as was also observed in corals treated with ash¹⁷ and Mn¹⁵. Dust supplementation however triggered a different species or holobiont-specific antioxidant response (Fig. 3). In *S. pistillata* treated with dust, we observed a significant increase in TAC and a slight downregulation in glutathione peroxidase and catalase activity, suggesting a change in antioxidant protection mechanisms. *T. reiniformis* showed an increase in catalase activity only at 32 °C dust conditions. Dust-derived metals and heat-stress may increase oxidative stress in corals¹⁶, with antioxidant protection expressed in TAC rather than in the glutathione peroxidase and catalase activities, enzymes involved in the degradation of H_2O_2 . Further studies need to be conducted to better understand the different antioxidant protection mechanisms at work in corals exposed to metals and heat-stress. Overall, the multiple lines of evidence indicate that natural non-biogenic nutrient deposition in seawater is benefiting coral photosynthesis through increased chlorophyll concentrations, regardless of the coral species. Dust provision also seem to affect antioxidant protective mechanisms by downregulating catalase and glutathione peroxidase activities and enhancing Total antioxidant capacity (TAC).

Benefits of Mn supplementation to corals are clear, on the contrary to iron

Dust provision brought essential metals to the Symbiodiniaceae of *S. pistillata*, in particular, Li, Mn and Fe, while also promoting photosynthesis. These 3 metals were highly collinear and were related to photophysiological proxies (specially chlorophyll a) of *S. pistillata*. This covariation indicates an interaction between these metals⁶². In plants, several transporter families, such as IRT1, IRT2, NRAMPs, and probably ZIP transport both Fe^{2+} and Mn^{2+} ^{62–64}. Homologues of ZIP and NRAMPs have also been identified in microalgae⁶⁵. In addition, both Mn⁶⁶ and Fe⁶⁷ deficiency is reported to induce transcription of AtNRAMP. It is therefore not surprising that Fe and Mn uptake may correlate each other since both stimulate the transcription of the same transporters. However, the correlation of those two metals with Li is not clear. Nevertheless, the collinearity of Li, Mn and Fe raises questions on which metal(s) plays a role in the photophysiology of Symbiodiniaceae. Research by Biscéré et

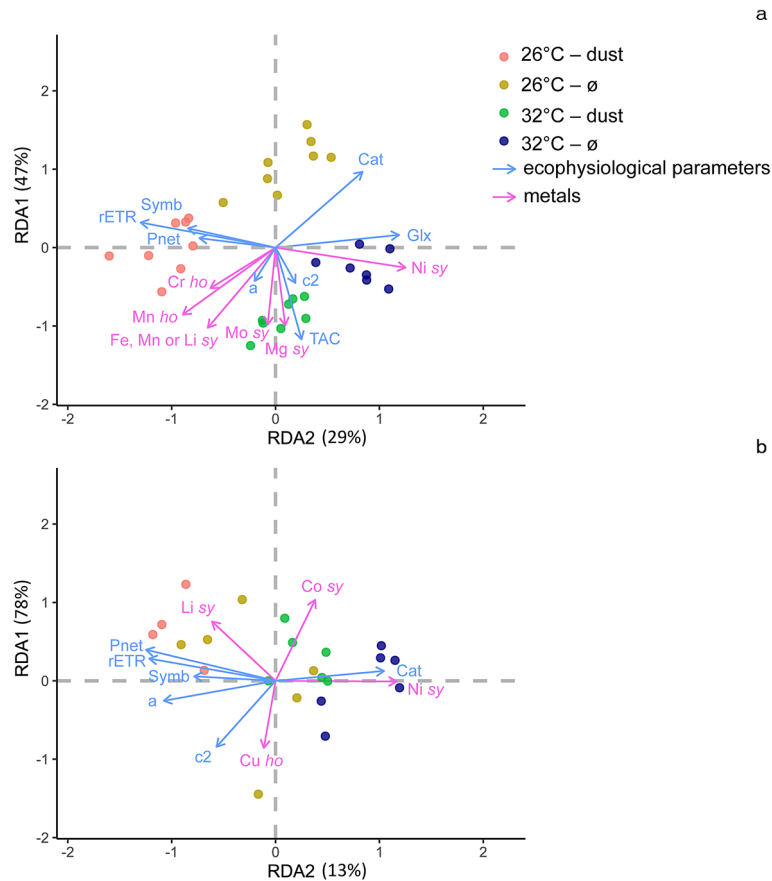


Fig. 9. RDA of the ecophysiological variables of (a) *S. pistillata* and (b) *T. reniformis*. The vectors of metal content significantly affecting ecophysiological variables are shown in pink (\rightarrow) (sy – in the symbionts; ho – in the host). The blue vectors (\rightarrow) represent the ecophysiological traits (rETR – Electron transport rate; Symb – symbionts density; P_{net} – net photosynthesis; a – chlorophyll a density; c2 – chlorophyll c2 density; Cat – catalase activity; TAC – Total antioxidant capacity). The length of the arrows indicates the contribution of each parameter to the axes.

al.¹⁵ and Förster et al.¹⁷ consistently showed the positive effects of manganese (Mn) supplementation on coral photosynthesis, chlorophyll content and relative electron transport rate (rETR). Also, previous studies have highlighted the role of Mn in enhancing the antioxidant response of corals⁶⁸. In particular, Mn contained in aerosol sources such as dust, fire, biogenic and volcanic ash has a high solubility that exceeds that of iron and several other metals in seawater¹⁹. Moreover, Mn has the potential to replace iron in the photosystem II (PSII) of symbionts^{12,69}. Thus, natural quantities of dust deposition may provide a mechanism to deliver significant amounts of Mn to corals and promote their resilience to thermal stress.

Iron has also been suggested to be an essential metal for cell functioning and stress responses in Symbiodiniaceae maintained under culture conditions¹² and its complete removal from seawater can quickly induce coral bleaching¹³. This is because iron enters the composition of several molecules involved in the photosynthetic chain, that are rapidly degraded under stress⁷⁰. The questions which remain are whether corals have sufficient iron under natural seawater concentrations for an optimal photosynthesis, whether they need more iron under thermal stress and which mechanisms are employed during iron uptake.

Despite the significant Fe uptake in *S. pistillata* supplied with dust, and the presumed uptake in *T. reniformis* (according to the observed isotopic change), the results from iron enrichment exposure did not enhance coral photosynthesis, under either normal or heat stress conditions. Indeed, our incubations of *S. pistillata* with dissolved iron alone showed no enhancement of coral photosynthesis, which is consistent with the studies of Biscéré et al.¹⁵ and Dellisanti et al.⁷¹. The role of iron in mitigating coral bleaching during thermal stress could be through its involvement in the composition of antioxidant enzymes^{62,67}, although Fe is also responsible for ROS production via the photo-Fenton like reaction⁷². In fact, dust-treated corals tended to have high TAC but low catalase activity, indicating that iron provided by dust is not enhancing antioxidant protective mechanism by catalase activity. Thus, the whole characterization of the antioxidant response of corals is necessary to understand the role of iron in enhancing this antioxidant response.

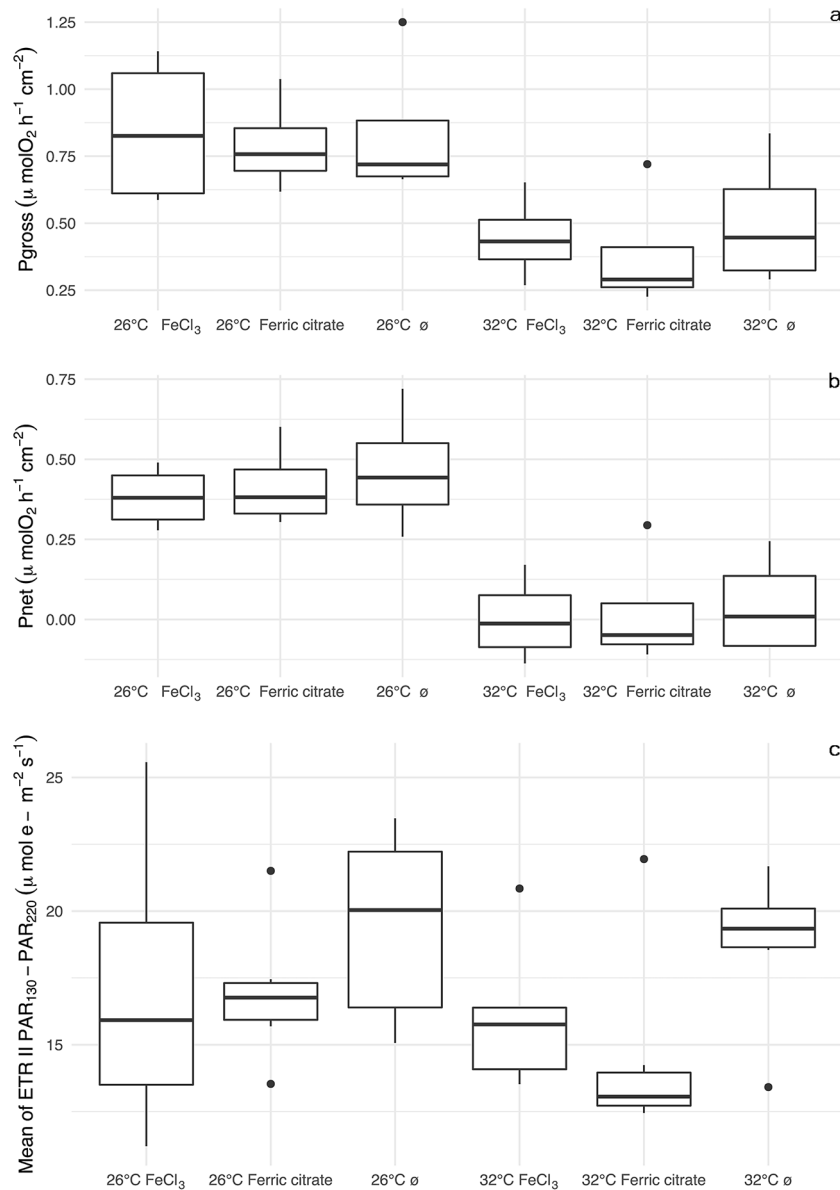


Fig. 10. Physiological and photosynthesis-related measurements in *S. pistillata*. Gross (a) and net photosynthesis (b), and electron transport rate at PAR₁₃₀-PAR₂₂₀ (rETR) (c) in *S. pistillata* exposed to iron chloride (FeCl₃), ferric citrate or nothing (ø), before (26 °C) and after thermal stress (32 °C).

Effect of thermal stress on the physiological response of corals maintained under control (non-dust) conditions

Thermal stress induced a significant bleaching (loss of Symbiodiniaceae) in both coral species, leading to a significant decrease in their rates of gross photosynthesis. Bleaching is common response of thermally-stressed corals and impairs their capacity to acquire autotrophic nutrients^{70,73}. *S. pistillata* is a species known for its resistance to heat stress up to 32 °C, which is however the tipping point of bleaching for this species⁷⁴.

Thermal stress also induced changes in the metalloome of symbionts and host of both coral species, but these changes were species and compartment (host/symbiont) dependent. Except for Fe, for which a previous study already showed a significant increase in the symbionts of *S. pistillata* under 30 °C¹⁶, the changes in the other metals need further investigations. There was finally a temperature effect on the isotopic signature of Fe, Cu and Zn in corals, which tended to increase at high temperatures. Similarly, a previous study showed that symbionts of heat stressed corals presented heavier *d*⁶⁶Zn and *d*⁶⁵Cu compared to control conditions, often independent of (heterotrophic) feeding¹⁴. Cu and Zn are structural or functional components of enzymes which are essential for redox reactions involved in respiration, such as electron transfer proteins, or oxidative stress, such as the superoxide dismutase⁷⁵. Preference to heavy Cu isotopes is already proved for an antioxidant enzyme⁷⁶ and for Cu-binding oxygen ligands (glutamate and aspartate), which are part of Cupro-proteins⁷⁷. Since these metals seem to not be limited in seawater, it is possible that their isotopic fractionation results from higher metal uptake

at high temperature preferentially incorporated into isotopically enriched proteins (redox or antioxidants), to support higher respiration rates and/or oxidative stress under heat stress. This scenario seems to be especially important for host compartments, as they were systematically enriched in ^{65}Cu under heat stress in both species. Further studies must be carried out to better understand which process fractionates Zn and Cu isotopes in different thermal conditions.

Conclusion

In summary, this study investigated the intricate relationship between desert dust supply, coral metallome, and the photophysiological response of two Red Sea scleractinian coral species, *Stylophora pistillata* and *Turbinaria reiniformis*, under thermal stress conditions. The results emphasized the important role of dust in the enrichment of coral hosts and symbionts with essential metals such as Li, Mn, Fe, Mg and Mo, which enhanced the photophysiological functions of corals under heat stress, especially in *S. pistillata*. Species-specific effects were evident as the two coral species responded differently to dust provision, indicating different requirements or capacities for metal uptake. Dust also led to a decrease of Ni uptake which in both species was anti correlated to photosynthesis, suggesting an enhancement of nitrogen assimilation via ammonium/nitrate uptake rather than urea uptake. Dust-derived iron is taken up by corals, but Fe^{3+} exposure (ferric chloride or ferric citrate) did not directly enhance photosynthesis, suggesting that it is the combination of metals released by dust that had a positive effect on coral photophysiology. Dust-treated corals differ from non-exposed corals by their Cu, Zn and Fe isotopic compositions. They were also distinguished by high total antioxidant capacity but low catalase and glutathione peroxidase activity, indicating that the whole characterization of the antioxidant response of corals coupled with stable isotopic compositions might appear as novel and unconventional methods helpful to better understand the role of dust in coral health. Overall, we suggest that desert dust may enhance the resistance of corals to bleaching, by increasing their photosynthesis likely due to metallomic changes in the symbionts. Furthermore, the results provide insights into the complex interactions between dust deposition, metallome dynamics and coral photophysiology and emphasize the importance of further research to fully understand the link between metal supplementation and corals to better understand their role on coral reef resilience.

Data availability

Datasets used during the current study are available from the corresponding author on reasonable request.

Received: 16 July 2024; Accepted: 22 October 2024

Published online: 03 November 2024

References

1. Odum, E. P. & Barrett, G. W. *Fundamentals of Ecology* (Saunders, 1971).
2. Muscatine, L. & Porter, J. W. Reef corals: mutualistic symbioses adapted to nutrient-poor environments. *BioScience*. **27**, 454–460 (1977).
3. LaJeunesse, T. C. et al. Systematic revision of Symbiodiniaceae highlights the antiquity and diversity of coral endosymbionts. *Curr. Biol.* **28**, 2570–2580 (2018).
4. Venn, A. A., Loram, J. E. & Douglas, A. E. Photosynthetic symbioses in animals. *J. Exp. Bot.* **59**, 1069–1080 (2008).
5. Davy, S. K., Allemand, D. & Weis, V. M. Cell biology of cnidarian-dinoflagellate symbiosis. *Microbiol. Mol. Biol. Rev.* **76**, 229–261 (2012).
6. Rädicker, N., Pogoreutz, C., Voolstra, C. R., Wiedenmann, J. & Wild, C. Nitrogen cycling in corals: the key to understanding holobiont functioning? *Trends Microbiol.* **23**, 490–497 (2015).
7. Hughes, T. P. et al. Spatial and temporal patterns of mass bleaching of corals in the Anthropocene. *Science*. **359**, 80–83 (2018).
8. Holbrook, N. J. et al. Keeping pace with marine heatwaves. *Nat. Rev. Earth Environ.* **1**, 482–493 (2020).
9. Houlbrèque, F., Ferrier-Pagès, C. Heterotrophy in tropical scleractinian corals. *Biol. Rev.* **84**, 1–7 (2009).
10. Reich, H. G., Camp, E. F., Roger, L. M. & Putnam, H. M. The trace metal economy of the coral holobiont: supplies, demands and exchanges. *Biol. Rev.* **98**, 623–642 (2023).
11. Rodriguez, I. B., Lin, S., Ho, J. & Ho, T. Y. Effects of trace metal concentrations on the growth of the coral endosymbiont *Symbiodinium kawagutii*. *Front. Microbiol.* **7**, 82 (2016).
12. Reich, H. G., Rodriguez, I. B., LaJeunesse, T. C. & Ho, T. Y. Endosymbiotic dinoflagellates pump iron: differences in iron and other trace metal needs among the Symbiodiniaceae. *Coral Reefs*. **39**, 915–927 (2020).
13. Shick, J. M. et al. Responses to iron limitation in two colonies of *Stylophora pistillata* exposed to high temperature: Implications for coral bleaching. *Limnol. Oceanogr.* **56**, 813–828 (2011).
14. Ferrier-Pagès, C., Sauzéat, L. & Balter, V. Coral bleaching is linked to the capacity of the animal host to supply essential metals to the symbionts. *Glob Change Biol.* **24**, 3145–3157 (2018).
15. Biscéré, T., Ferrier-Pagès, C., Gilbert, A., Pichler, T. & Houlbrèque, F. Evidence for mitigation of coral bleaching by manganese. *Sci. Rep.* **8**, 16789 (2018a).
16. Blanckaert, A. C., Omanović, D., Fine, M., Grover, R. & Ferrier-Pagès, C. Desert dust deposition supplies essential bioelements to Red Sea corals. *Glob Change Biol.* **28**, 2341–2359 (2022).
17. Förster, F. et al. Increased coral biomineralization due to enhanced symbiotic activity upon volcanic ash exposure. *Sci. Total Environ.* **912**, 168694 (2024).
18. Prakash, P. J., Stenichkov, G., Kalenderski, S., Osipov, S. & Bangalath, H. The impact of dust storms on the Arabian Peninsula and the Red Sea. *Atmos. Chem. Phys.* **15**, 199–222 (2015).
19. Mahowald, N. M. et al. Aerosol trace metal leaching and impacts on marine microorganisms. *Nat. Commun.* **9**, 2614 (2018).
20. Reichelt-Brushett, A. J. & Harrison, P. L. The effect of selected trace metals on the fertilization success of several scleractinian coral species. *Coral Reefs*. **24**, 524–534 (2005).
21. Shaltout, M. Recent sea surface temperature trends and future scenarios for the Red Sea. *Oceanologia*. **61**, 484–504. <https://doi.org/10.1016/j.oceano.2019.05.002> (2019).
22. Kessler, N. et al. Selective collection of iron-rich dust particles by natural *Trichodesmium* colonies. *ISME J.* **14**, 91–103 (2019).
23. Stimson, J. & Kinzie, I. I. The temporal pattern and rate of release of zooxanthellae from the reef coral *Pocillopora damicornis* (Linnaeus) under nitrogen-enrichment and control conditions. *J. Exp. Mar. Biol. Ecol.* **153**, 63–74 (1991).
24. Jeffrey, S. T. & Humphrey, G. F. New spectrophotometric equations for determining chlorophylls a, b, c1 and c2 in higher plants, algae and natural phytoplankton. *Biochem. Physiol. Pflanz.* **167**, 191–194 (1978).

25. Maréchal, C. N., Télouk, P. & Albarède, F. Precise analysis of copper and zinc isotopic compositions by plasma-source mass spectrometry. *Chem. Geol.* **156**, 251–273 (1999).
26. Poitrasson, F. & Freyrier, R. Heavy iron isotope composition of granites determined by high resolution MC-ICP-MS. *Chem. Geol.* **222**, 132–147 (2005).
27. Sauzéat, L. et al. Inter-comparison of stable iron, copper and zinc isotopic compositions in six reference materials of biological origin. *Talanta*. **221**, 121576 (2021).
28. Costas-Rodríguez, M. et al. Isotopic analysis of Cu in blood serum by multi-collector ICP-mass spectrometry: a new approach for the diagnosis and prognosis of liver cirrhosis? *Metallomics*. **7**, 491–498 (2015).
29. Oakes, K. D. & van Der Kraak, G. J. Utility of the TBARS assay in detecting oxidative stress in white sucker (*Catostomus commersoni*) populations exposed to pulp mill effluent. *Aquat. Toxicol.* **63**, 447–463 (2003).
30. Bradford, M. M. A rapid and sensitive method for the quantitation of microgram quantities of protein utilizing the principle of protein-dye binding. *Anal. Biochem.* **72**, 248–254 (1976).
31. Ter Braak, C. J. The analysis of vegetation-environment relationships by canonical correspondence analysis. *Vegetation*. **69**, 69–77 (1987).
32. Ter Braak, C. J. Canonical community ordination. Part I: Basic theory and linear methods. *Ecoscience*. **1**, 127–140 (1994).
33. Polle, A. Dissecting the superoxide dismutase-ascorbate-glutathione-pathway in chloroplasts by metabolic modeling. Computer simulations as a step towards flux analysis. *Plant. Physiol.* **126**, 445–462 (2001).
34. Krueger, T. et al. Transcriptomic characterization of the enzymatic antioxidants FeSOD, MnSOD, APX and KatG in the dinoflagellate genus *Symbiodinium*. *BMC Evo Biol.* **15**, 1–20 (2015).
35. Levin, R. A. et al. Sex, scavengers, and chaperones: transcriptome secrets of divergent *Symbiodinium* thermal tolerances. *Mol. Biol. Evo.* **33**, 2201–2215 (2016).
36. Goyen, S. et al. A molecular physiology basis for functional diversity of hydrogen peroxide production amongst *Symbiodinium* spp. (Dinophyceae). *Mar. Biol.* **164**, 1–2 (2017).
37. Mass, T. et al. Photoacclimation of *Stylophora pistillata* to light extremes: metabolism and calcification. *Mar. Ecol. Prog Ser.* **334**, 93–102 (2007).
38. Martínez, S. et al. Energy sources of the depth-generalist mixotrophic coral *Stylophora pistillata*. *Front. Mar. Sci.* **7**, 566663 (2020).
39. Buitrago-López, C. et al. Disparate population and holobiont structure of pocilloporid corals across the Red Sea gradient demonstrate species-specific evolutionary trajectories. *Mol. Ecol.* **32**, 2151–2173 (2023).
40. Ezzat, L., Fine, M., Maguer, J. F., Grover, R. & Ferrier-Pages, C. Carbon and nitrogen acquisition in shallow and deep holobionts of the scleractinian coral *S. pistillata*. *Front. Mar. Sci.* **13**, 102 (2017).
41. Conway, T. M. et al. Tracing and constraining anthropogenic aerosol iron fluxes to the North Atlantic Ocean using iron isotopes. *Nat. Commun.* **10**, 2628 (2019).
42. Ellwood, M. J. et al. Distinct iron cycling in a Southern Ocean eddy. *Nat. Commun.* **11**, 825 (2020).
43. Wu, B., Amelung, W., Xing, Y., Bol, R. & Berns, A. E. Iron cycling and isotope fractionation in terrestrial ecosystems. *Earth-Sci. Rev.* **190**, 323–352 (2019).
44. Sun, R. & Wang, B. Iron isotope fractionation during uptake of ferrous ion by phytoplankton. *Chem. Geol.* **481**, 65–73 (2018).
45. Mulholland, D. S. et al. Iron isotope fractionation during Fe (II) and Fe (III) adsorption on cyanobacteria. *Chem. Geol.* **400**, 24–33 (2015).
46. Swanner, E. D. et al. Iron isotope fractionation during Fe (II) oxidation mediated by the oxygen-producing marine cyanobacterium *Synechococcus* PCC 7002. *Env. Sci. Technol.* **5**, 4897–4906 (2017).
47. Albarède, F. The stable isotope geochemistry of copper and zinc. *Rev. Mineral. Geochem.* **55**, 409–427 (2004).
48. Köbberich, M. & Vance, D. Zn isotope fractionation during uptake into marine phytoplankton: implications for oceanic zinc isotopes. *Chem. Geol.* **523**, 154–161 (2019).
49. Schleicher, N. J. et al. A global assessment of copper, zinc, and lead isotopes in mineral dust sources and aerosols. *Front. Earth Sci.* **8**, 167 (2020).
50. Maréchal, C. N., Nicolas, E., Douchet, C. & Albarède, F. Abundance of zinc isotopes as a marine biogeochemical tracer. *Geochem. Geophys. Geosyst.* **1**, 1515 (2000).
51. Ban, Y., Aida, M., Nomura, M. & Fujii, Y. Zinc isotope separation by ligand exchange chromatography using cation exchange resin. *J. Ion Exch.* **13**, 46–52 (2002).
52. Ding, X., Nomura, M. & Fujii, Y. Zinc isotope effects by chromatographic chelating exchange resin. *Prog Nucl. Energy.* **52**, 164–167 (2010a).
53. Ding, X., Nomura, M., Suzuki, T. & Fujii, Y. Chromatographic zinc isotope separation by chelating exchange resin. *Chromatogr.* **71**, 195–199 (2010b).
54. Markovic, T. et al. Experimental determination of zinc isotope fractionation in complexes with the phytosiderophore 2'-deoxymugenic acid (DMA) and its structural analogues, and implications for plant uptake mechanisms. *Environ. Sci. Technol.* **51**, 98–107 (2017).
55. Weldeghebriel, M. F. & Lowenstein, T. K. Seafloor hydrothermal systems control long-term changes in seawater [Li⁺]: Evidence from fluid inclusions. *Sci. Adv.* **9**, eadf1605 (2023).
56. Steiner, Z. et al. Variability in the concentration of lithium in the Indo-Pacific Ocean. *Global Biogeochem. Cy.* **36**, e2021GB007184 (2022).
57. Rollion-Bard, C. et al. Effect of environmental conditions and skeletal ultrastructure on the Li isotopic composition of scleractinian corals. *Earth Planet. Sci. Lett.* **286**, 63–70 (2009).
58. Roux, M. & Dosseto, A. From direct to indirect lithium targets: a comprehensive review of omics data. *Metallomics*. **9**, 1326–1351 (2017).
59. Grover, R., Maguer, J. F., Allemand, D. & Ferrier-Pagès, C. Urea uptake by the scleractinian coral *Stylophora pistillata*. *J. Exp. Mar. Biol. Ecol.* **332**, 216–250 (2006).
60. Dupont, C. L., Buck, K. N., Palenik, B. & Barbeau, K. Nickel utilization in phytoplankton assemblages from contrasting oceanic regimes. *Deep Sea Res. I: Oceanogr. Res. Pap.* **57**, 553–566 (2010).
61. Biscéré, T. et al. Enhancement of coral calcification via the interplay of nickel and urease. *Aquat. Toxicol.* **200**, 247–256 (2018b).
62. Rai, S., Singh, P. K., Mankotia, S., Swain, J. & Satbhai, S. B. Iron homeostasis in plants and its crosstalk with copper, zinc, and manganese. *Plant. Stress.* **1**, 100008 (2021).
63. Grotz, N. & Guerinot, M. L. Molecular aspects of Cu, Fe and Zn homeostasis in plants. *Biochim. Biophys. Acta - Mol. Cell. Res.* **1763**, 595–608 (2006).
64. Lelandais, G. et al. *Ostreococcus tauri* is a new model green alga for studying iron metabolism in eukaryotic phytoplankton. *BMC Genom.* **17**, 1–23 (2016).
65. Gao, X., Bowler, C. & Kazamia, E. Iron metabolism strategies in diatoms. *J. Exp. Bot.* **72**, 2165–2180 (2021).
66. Ramirez, L., Graziano, M. & Lamattina, L. Decoding plant responses to iron deficiency: is nitric oxide a central player? *Plant. Signal. Behav.* **3**, 795–797 (2008).
67. Guerinot, M. L. Microbial iron transport. *Annu. Rev. Microbiol.* **48**, 743–772 (1994).
68. Montalbetti, E. et al. Manganese benefits heat-stressed corals at the cellular level. *Front. Mar. Sci.* **8**, 681119 (2021).
69. Raven, J. A., Evans, M. C. & Korb, R. E. The role of trace metals in photosynthetic electron transport in O₂-evolving organisms. *Photosynth Res.* **60**, 111–150 (1999).

70. Suggett, D. J. & Smith, D. J. Coral bleaching patterns are the outcome of complex biological and environmental networking. *Glob Change Biol.* **26**, 68–79 (2020).
71. Dellisanti, W., Zhang, Q., Ferrier-Pagès, C. & Kühl, M. Contrasting effects of increasing dissolved iron on photosynthesis and O₂ availability in the gastric cavity of two Mediterranean corals. *PeerJ.* **12**, e17259 (2024).
72. Morris, J. J., Rose, A. L. & Lu, Z. Reactive oxygen species in the world ocean and their impacts on marine ecosystems. *Redox Biol.* **52**, 102285 (2022).
73. Ainsworth, T. D. & Brown, B. E. Coral bleaching. *Curr. Biol.* **31**, R5–R6 (2021).
74. Evensen, N. R., Fine, M., Perna, G., Voolstra, C. R. & Barshis, D. J. Remarkably high and consistent tolerance of a Red Sea coral to acute and chronic thermal stress exposures. *Limnol. Oceanogr.* **66**, 1718–1729 (2021).
75. Bremner, I. & H Beattie, J. Copper and zinc metabolism in health and disease: speciation and interactions. *Proc. Nutr. Soc.* **54**, 489–499 (1995).
76. Larner, F., McLean, C. A., Halliday, A. N. & Roberts, B. R. Copper isotope compositions of superoxide dismutase and metallothionein from post-mortem human frontal cortex. *Inorganics.* **7**, 86 (2019).
77. Selden, C. R., Schilling, K., Godfrey, L. & Yee, N. Metal-binding amino acid ligands commonly found in metalloproteins differentially fractionate copper isotopes. *Sci. Rep.* **14**, 1902 (2024).

Acknowledgements

We thank Cécile Rottier for laboratory assistance and Dominique Desgre for assistance on handling the corals colonies. This study has been co-funded by CORDAP (Coral Research and Development Accelerate Platform) on the project: “Super supplement: boosting coral resilience through nutritional supplements.

Author contributions

C.F.P., K.A., R.G. designed the study; C.F.P., D.O., K.A., L.S., R.G., M.F., M.I.M.N. contributed to theoretical concepts applied in the study; C.F.P., K.A., R.G. carried out the experiments; D.O., K.A., L.S., M.I.M.N. processed the samples; C.F.P., K.A., L.S. analysed the data; K.A. wrote the article with contributions from C.F.P., D.O., L.S., M.F.; all the authors contributed to the revision of the paper.

Declarations

Competing interests

The authors declare no competing interests.

Additional information

Supplementary Information The online version contains supplementary material available at <https://doi.org/10.1038/s41598-024-77381-y>.

Correspondence and requests for materials should be addressed to K.A. or C.F.-P.

Reprints and permissions information is available at www.nature.com/reprints.

Publisher’s note Springer Nature remains neutral with regard to jurisdictional claims in published maps and institutional affiliations.

Open Access This article is licensed under a Creative Commons Attribution-NonCommercial-NoDerivatives 4.0 International License, which permits any non-commercial use, sharing, distribution and reproduction in any medium or format, as long as you give appropriate credit to the original author(s) and the source, provide a link to the Creative Commons licence, and indicate if you modified the licensed material. You do not have permission under this licence to share adapted material derived from this article or parts of it. The images or other third party material in this article are included in the article’s Creative Commons licence, unless indicated otherwise in a credit line to the material. If material is not included in the article’s Creative Commons licence and your intended use is not permitted by statutory regulation or exceeds the permitted use, you will need to obtain permission directly from the copyright holder. To view a copy of this licence, visit <http://creativecommons.org/licenses/by-nc-nd/4.0/>.

© The Author(s) 2024